Cholesterol Oxidase Senses Subtle Changes in Lipid Bilayer Structure[†]

Kwang-wook Ahn and Nicole S. Sampson*

Department of Chemistry, State University of New York, Stony Brook, New York 11794-3400

Received September 19, 2003; Revised Manuscript Received November 14, 2003

ABSTRACT: We investigated the dependence of cholesterol oxidase catalytic activity and membrane affinity on lipid structure in model membrane bilayers. The binding affinities of cholesterol oxidase to 100-nm unilamellar vesicles composed of mixtures of DOPC or DPPC and cholesterol are not sensitive to cholesterol mole fraction if the phase of the membrane is in a fluid state. When the membrane is in a solid-ordered state, the binding affinity of cholesterol oxidase increases approximately 10-fold. The second-order rate constants (k^*_{cat}/K^*_m) for different lipid mixtures show a 2-fold substrate specificity for cholesterol in the l_d phase of high cholesterol chemical activity over cholesterol in the l_o phase. Moreover, the enzyme is 2-fold more specific for cholesterol in the l_o phase than in the s_o phase. Likewise, there is 2-fold substrate specificity for the high cholesterol chemical activity l_d phase over the low chemical activity l_d phase. The specificities for the l_d phase of low cholesterol chemical activity and the l_o phase are the same. These data indicate that the more ordered the lipid cholesterol structure in the bilayer, the lower the catalytic rate. However, under all of the conditions investigated, the enzyme is never saturated with substrate. The enzymatic activity directly reflects the facility with which cholesterol can move out of the membrane, whether changes in cholesterol transfer facility are due to phase changes or more localized changes in packing. We conclude that the activity of cholesterol oxidase is directly and sensitively dependent on the physical properties of the membrane in which its substrate is bound.

Cholesterol oxidase (EC 1.1.3.6) is a monomeric enzyme that catalyzes the two step conversion of cholesterol to cholest-4-en-3-one using an FAD[1] cofactor (Scheme 1). The first step of the reaction catalyzed is cholesterol oxidation utilizing a tightly bound FAD molecule to produce H_2O_2 and cholest-5-en-3-one. The second step is isomerization of cholest-5-en-3-one to produce the final product, cholest-4-en-3-one. This enzyme is used clinically to determine serum cholesterol concentrations and is also being developed as an insecticide due to its larvicidal properties (*1*, *2*). In nonpathogenic bacteria, e.g., *Streptomyces*, this enzyme is secreted and is part of a bacterial metabolic pathway for utilizing cholesterol as a carbon source. In pathogenic bacteria, e.g., *Rhodococcus* and slow-growing *Mycobacteria*, the enzyme is required for infection of the host macrophage (*3*−*5*). Cholesterol oxidase's role as a virulence factor is related to its ability to alter the physical structure of lipid membranes. Its membrane structure altering characteristics have also led to its use in studying cell membranes and the importance of cholesterol in the function of lipid rafts in signal transduction (*6*).

Scheme 1: Reaction Catalyzed by Cholesterol Oxidase

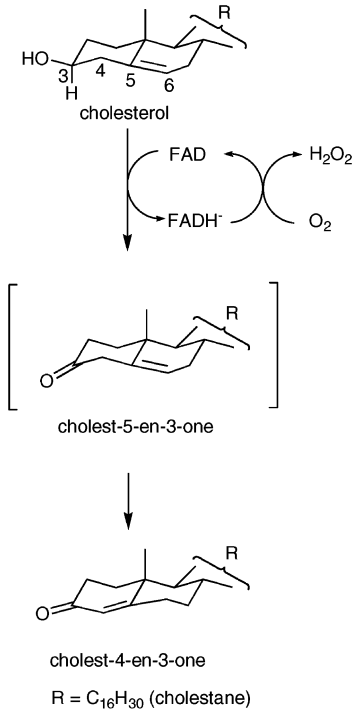

Cholesterol oxidase is water-soluble; however, the cholesterol substrate is integrated in the lipid bilayer of the cell membrane. Thus, the enzyme must either wait for cholesterol to partition out of the membrane and bind it from aqueous solution, or the enzyme must associate with the membrane to allow direct partitioning of cholesterol from the membrane

[†] Financial support from the National Institutes of Health (HL53306, N.S.S.) and the Rotary Club Foundation (K.A.) is gratefully acknowledged.

* To whom correspondence should be addressed. E-mail: nicole.sampson@stonybrook.edu. Phone: (631) 632-7952. FAX: (631) 632-5731.

[1] Abbreviations: BSA, bovine serum albumin; DOPC, 1,2-dioleoyl-*sn*-glycero-3-phosphatidylcholine; DPPC, 1,2-dipalmitoyl-2-oleoyl-*sn*-glycero-3-phosphatidylcholine; ePC, egg phosphatidylcholine; FAD, flavin adenine dinucleotide; MUV, medium-sized unilamellar vesicle; POPC, 1-palmitoyl-2-oleoyl phosphatidylcholine; T_m, melting temperature; s_o, solid-ordered; l_o, liquid-ordered; l_d, liquid-disordered.

10.1021/bi035697q CCC: $27.50
Published on Web 12/24/2003

into the active site. Since the rate of enzymatic turnover is faster than the rate of cholesterol release from a lipid bilayer (*7*), the enzyme must associate with the membrane before binding substrate in the active site (*8*). Our current hypothesis based on binding (*9*), mutagenesis (*8*), and vesicle leakage data (*10*) is that the physical association of cholesterol oxidase with the bilayer does not perturb the membrane structure. Rather, the enzyme provides a hydrophobic binding cavity that allows favorable partitioning of the cholesterol from the membrane into the enzyme. This suggests that cholesterol oxidase activity should be sensitive to the inherent stability of cholesterol in the membrane and can be used as a sensor of bilayer lipid phase. In fact, experiments with monolayers suggest that it is. In monolayers, cholesterol oxidase activity appears to depend on the strength of the cholesterol/phospholipid interaction in the monolayer (*11*−*16*), and it correlates to rates observed with vesicle bilayers (*17*). These experiments were primarily conducted with high cholesterol/phospholipid ratios, i.e., between 0.3:1 and 1:1. Moreover, these activity measurements did not take into account the effects that the interfacial nature of the enzyme, and thus its affinity for the membrane surface, may have on the observed rate. Here we present our investigation of how cholesterol oxidase activity depends on the lipid phase of the membrane bilayer into which the cholesterol is incorporated at mole fractions ranging from 0 to 0.5 cholesterol, and we include an analysis of binding affinities. Furthermore, we have adapted a kinetic paradigm that allows comparison of rates from membranes with different mole fractions of cholesterol.

In biological membranes, the most abundant lipid components, in addition to cholesterol, are polar lipids such as phospholipids and sphingolipids which form the lipid bilayer. Many studies with model membranes have revealed that the lipid bilayer may exist in different phases, i.e., the solidlike gel state (s_o), in which the lipid molecules are tightly packed and highly ordered with each respect to each other and have restricted lateral motion, and the liquidlike fluid state (l_d), in which lipid molecules are disordered and in considerable motion (*18*). Cholesterol further affects the phase behavior of the lipid bilayer.

Studies of the phase behavior of cholesterol/phospholipid binary mixtures have indicated that an intermediate state called the liquid-ordered (l_o) state forms (*19*−*23*). The l_o state is a cholesterol-enriched phase exhibiting intermediate physical properties between the solid-ordered (s_o) and liquid-disordered (l_d) phases, characterized by both rapid lateral diffusion yet tight packing of lipid molecules. In addition, in binary mixtures there is a region of l_o/l_d immiscibility in which both phases are present. Lipid rafts are proposed to be small domains of l_o lipid within the cell membrane (*24*). We initiated our investigation into the dependence of cholesterol oxidase activity on membrane phase using model binary membrane systems with known phase order to see if the enzyme could distinguish between these different phases.

We investigated the dependence of cholesterol oxidase activity on bilayer lipid phase by monitoring the initial velocities of wild-type *Streptomyces sp. SA-COO* cholesterol oxidase activity on medium-sized (100 nm diameter) unilamellar vesicles (MUVs) made of phosphatidyl cholines and varying amounts of cholesterol. We used two kinds of phosphatidyl choline: dioleoylphosphatidyl choline (DOPC, $T_m = -18$ °C) and dipalmitoylphosphatidyl choline (DPPC, $T_m = 41$ °C) (*25*). These lipids have different chain lengths, degrees of saturation, and T_m's, and cover the range of phase behaviors described above. In addition, we directly monitored binding to the lipid bilayer using a catalytically inactive, but folded, mutant, H447E/E361Q (*26*). Our results demonstrate that not only is the enzyme activity and affinity sensitive to lipid phase, but it also detects changes in cholesterol chemical activity in the membrane.

EXPERIMENTAL METHODS

Materials. Cholesterol and horseradish peroxidase were purchased from Sigma Chemical Company (St. Louis, MO). Lipids were purchased from Avanti Polar Lipids (Alabaster, AL). Radiolabeled lipids were purchased from NEN Life Sciences (Boston, MA). The plasmids for heterologous expression of *Streptomyces sp. SA-COO* wild-type cholesterol oxidase, pCO202, and H447E/E361Q mutant cholesterol oxidase, pCO233, and purification have been described previously (*26*, *27*). Unless otherwise specified, all chemicals and solvents, of reagent or HPLC grade, were supplied by Fisher Scientific (Pittsburgh, PA). Water for assays and chromatography was distilled, followed by passage through a Barnstead NANOpure filtration system to give a resistivity better than 18 MΩ.

General Methods. Vesicles were prepared with an extruder from Lipex Biomembranes Inc. (Vancouver, BC, Canada). A Shimadzu UV2101 PC Spectrophotometer or Molecular Devices Spectramax^{plus} multichannel microplate spectrophotometer (Sunnyvale, CA) was used for assays. Fluorescence measurements were taken on a Spex Fluorolog 3-21 fluorimeter. A Proterion DynaPro light scattering spectrometer (Piscataway, NJ) was used for light scattering measurements. A Beckman liquid scintillation counter (Type LS 5801) was used for measuring radioactivity. The buffers used were A: 50 mM sodium phosphate, pH 7.0; B: 50 mM sodium phosphate, pH 7.0, 0.020% (w/v) BSA; C: 50 mM sodium phosphate, pH 7.0, 0.020% (w/v) BSA, 0.025% (w/v) Triton X-100.

Preparation of Lipid Vesicles. Medium, 100-nm unilamellar vesicles were made from mixtures of lipids using extrusion (*28*). Lipids (10 μmol) were mixed as $CHCl_3$ solutions in a round-bottomed flask, dried as a thin film under reduced pressure in a rotary evaporator for 20 min, and evacuated under high vacuum for 2 h. The lipid was resuspended in 1 mL of buffer A with vortexing. Five freeze−thaw cycles, at −80 and 37 °C, followed by 10 extrusion cycles through two stacked 100-nm filters (Costar, Cambridge, MA) using a nitrogen gas pressure of 350−400 psi, provided a homogeneous batch of vesicles as determined by light scattering. Light scattering measurements were made using 30 μM phospholipid vesicle solutions in buffer A. Phospholipid concentrations of vesicle solutions were measured by the Stewart assay (*29*). Wild-type cholesterol oxidase was used to determine total cholesterol concentration in vesicles after lysing vesicles with 0.1% Triton X-100.

Preparation of Radiolabeled Vesicles. Donor vesicles (0.55 mM, total lipid concentration) contained a trace of [4-^{14}C]-labeled cholesterol (1 μCi) as a transferable lipid and included *N*-palmitoyl-dihydrolactocerebroside for agglutination with lectin, with a total mole ratio of eggPC/cerebroside/sterol =

42.5:7.5:50. Control donor vesicles were prepared with a trace of [oleate-1-^{14}C]-labeled cholesteryl oleate (1 μCi), with the same mole ratio of eggPC/cerebroside/sterol. Acceptor vesicles (10 mM, total lipid concentration), that contained [cholesteryl-1,2-^{3}H(N)]-labeled cholesteryl hexadecyl ether (1 μCi) as a nonexchangeable marker, were composed of eggPC/steroid = 50:50. A total of 800 μL of donor stock was diluted to 2.05 mL in buffer A and extruded 10 times through two stacked 100 nm filters. A total of 550 μL of acceptor stock solution (10 mM) was diluted to 1.80 mL in buffer A.

Measurement of the Rate of [^{14}C]-Labeled Cholesterol Transfer. After extrusion, 1.5 mL each of extruded donor and acceptor vesicle solutions were mixed and vortexed for 15−20 s, and 10 aliquots (200 μL) of the mixture were prepared in Eppendorf centrifuge tubes (0.5 mL) and incubated at 37 °C. Separation of donor and acceptor vesicles was achieved by adding 7.5 μg of lectin (from *Ricinus Communis*, RCA_{120}, Sigma) to each Eppendorf tube at various time intervals, followed by vortexing and centrifugation for 15−20 min at room temperature. A total of 150 μL of the supernatant was removed to a scintillation vial, 5 mL of scintillation fluid (Scintiverse* II) was added to the tube and the tube shaken for 20−30 s. The dpm ratio of [^{14}C]/[^{3}H] for each vial was determined by liquid scintillation counting. The control experiments were carried out using the same protocol described above, except the donor vesicles contained [^{14}C]-labeled cholesteryl oleate.

Fluorescence Binding Measurements (*9*). Binding of cholesterol oxidase to vesicles was assayed by monitoring the change in tryptophan fluorescence. All binding assays were conducted in buffer A. The instrument was operated in the ratio-recording mode. One-centimeter path length cuvettes were used. Samples were stirred during the assay to prevent the settling of the protein. The cuvettes were washed with nitric acid before each assay. Filters (320-nm cut-on) were placed before the emission monochromator to eliminate any contribution from scattered light.

Tryptophan was excited at 280 nm, and the emission spectrum was acquired from 320 to 450 nm with a 1-nm excitation slit and a 3-nm emission slit. Sample signals were corrected for light fluctuations by simultaneously monitoring the exciting light on a reference photomultiplier. Protein (5 μg/mL) was titrated with increasing amounts of lipid vesicles (0−150 μL of a 3 mM stock solution) to a final concentration of 700 μM with constant stirring. Emission was corrected for any background signal by performing a titration in the absence of protein.

Binding constants were analyzed by first correcting spectra for dilution and background signal. The spectra were integrated and normalized to their value in the absence of added lipid. The binding isotherm was fitted to the following equation using KaleidaGraph software (Synergy Software, Vermont, USA):

$$\Delta F = (\Delta F_{max}[L])/([L] + K_d) \quad (1)$$

[L], monomeric lipid concentration; K_d, dissociation constant; ΔF, change in fluorescence intensity; ΔF_{max}, maximum change in fluorescence intensity.

Activity Assay of Cholesterol Oxidase with Vesicles. The activity of wild-type cholesterol oxidase was measured by following the appearance of conjugated enone at 240 nm (ϵ_{240} = 12 100 M^{-1} cm^{-1} (*30*)). The enzyme stock solution was diluted with buffer B. A total of 980−990 μL of vesicle solutions in buffer B was added to a quartz cuvette with a 10-mm path length and equilibrated for 10−15 min. A total of 10 μL (10−100 ng) of wild-type cholesterol oxidase was added and the absorbance at 240 nm corresponding to the first 10% of total cholesterol conversion was measured as a function of time. In the case of DOPC/cholesterol vesicles, 10 μL of catalase (2.1 U/μL) was added before addition of wild-type cholesterol oxidase to prevent the undesired peroxidation of double bonds in the acyl chains.

The activity was also determined using a horseradish peroxidase coupled assay to quantitate the rate of formation of H_2O_2. The H_2O_2 formation was followed by excitation at 325 nm and monitoring the fluorescence emission at 415 nm (slits = 1.5 nm). The standard assay conditions were the same as the A_{240} assay, except that 1.0 mM *p*-hydroxyphenylacetic acid and 10 units of horseradish peroxidase were added before adding enzyme. Independent sets of data were fit simultaneously to a binding isotherm using Kaleidagraph:

$$v_i = (v_i^{sat}[L])/(K_{app} + [L]) \quad (2)$$

v_i, initial rate; v_i^{sat}, v_i when cholesterol oxidase binding to the vesicle is saturated; K_{app}, apparent K_d for coupled equilibrium of binding of enzyme to vesicle and of binding substrate to the enzyme; [L], monomeric lipid concentration that is proportional to the number of vesicles added.

RESULTS

Reaction Progress Curves. The activity of wild-type cholesterol oxidase was monitored using two assays. The kinetic activity was directly measured by monitoring UV absorbance of cholest-4-en-3-one, the isomerization product, as a function of time. The same steady-state rates were measured by following the rate of product H_2O_2 formation using a horseradish peroxidase coupled assay. This assay was used to follow product formation by the E361Q mutant that produces cholest-5-en-3-one as the product or for improved sensitivity of monitoring wild-type reactions on slow substrates.

Product formation versus time was monitored for both wild type and the E361Q mutant (Figure 1A,B) using the horseradish peroxidase assay. The activity profile for wild type is sigmoidal; for E361Q, it is hyperbolic. These reaction progress curves suggested that the presence of the reaction product alters the catalytic rate constants of the enzyme. To test whether the hyperbolic behavior of E361Q was due to the absence of cholest-4-en-3-one, we next compared the initial rates for reaction of E361Q in 100 nm vesicles composed of ePC/steroid (1:1) that contained either 15 mol % cholest-4-en-3-one (ePC/cholesterol/cholest-4-en-3-one, 50:35:15) or 15 mol % cholest-5-en-3-one (ePC/cholesterol/cholest-5-en-3-one, 50:35:15). The initial rate for oxidation of 35 mol % cholesterol was 2.2-fold faster in the presence of the cholest-4-en-3-one than in the presence of cholest-5-en-3-one. This reaction rate difference confirmed that the presence of cholest-4-en-3-one increases the catalytic rate constant of both wild type and mutant enzyme. This could be through alteration of the lipid bilayer structure or activation of the enzyme.

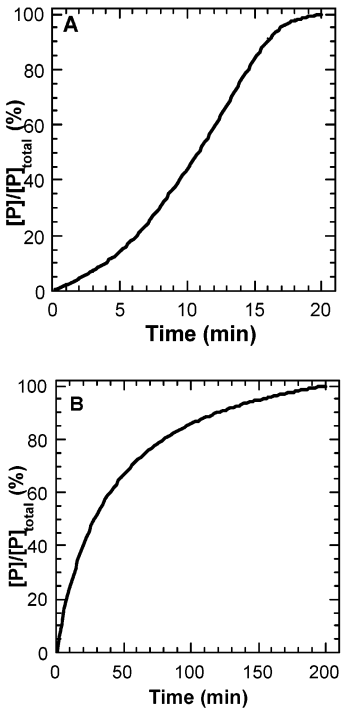

FIGURE 1: (A) Reaction progress curves observed for the turnover of substrate in vesicles. Wild-type cholesterol oxidase (1.29 μg/mL) and ePC/cholesterol vesicles (1:1, 32 μM in ePC). (B) E361Q cholesterol oxidase (7.9 μg/mL) and ePC/cholesterol vesicles (1:1, 50 μM in ePC).

Dependence of the Rate of Cholesterol Transfer on Mole Fraction of Cholest-4-en-3-one. The rate of cholesterol transfer between vesicles was measured using the method of Hope (*28*) to monitor the effect of cholest-4-en-3-one, a product of the reaction catalyzed by cholesterol oxidase, on steroid-lipid packing in the lipid bilayer. Vesicles were prepared as 100-nm medium, unilamellar vesicles (MUV) using extrusion, in a 1:1 ratio of ePC and steroid (mixture of cholesterol and cholest-4-en-3-one). Donor vesicles contained [^{14}C]-labeled cholesterol as a transferable lipid and also included *N*-palmitoyldihydrolactocerebroside for separation of the donor vesicles from acceptor vesicles by lectin-mediated agglutination. Acceptor vesicles contained [^{3}H]-labeled cholesteryl hexadecyl ether as a nonexchangeable marker.

We measured the half-life ($t_{1/2}$) for cholesterol transfer from donor vesicles to acceptor vesicles as a function of cholest-4-en-3-one mole fraction in the absence of cholesterol oxidase (Table 1). We observed that the $t_{1/2}$ of cholesterol transfer decreased when the mole fraction of cholest-4-en-3-one in the lipid bilayer increased (Figure 2). Control experiments with donor vesicles containing [^{14}C]-labeled cholesteryl oleates showed that precipitation by agglutination was quantitative, that no significant transfer of [^{3}H]-labeled cholesteryl hexadecyl ether from acceptor to donor vesicles occurred, and that the dihydrolactocerebroside tag does not exchange, as expected (data not shown). Thus, the rate of cholesterol transfer out of the donor vesicle membrane increases with increasing ratios of cholest-4-en-3-one in the vesicle membrane. Assays using vesicles with POPC/steroid (1:1) under the same conditions gave the same result. Cholest-4-en-3-one alters the lipid bilayer affinity for cholesterol, and thus can indirectly alter the catalytic rate of cholesterol oxidase. This suggested that the catalytic rates would be sensitive to other changes in lipid−cholesterol interactions. Moreover, it was necessary to monitor catalytic activity using initial rates rather than full reaction curves.

Table 1: Half-Lives of Cholesterol Transfer between Vesicle Membranes[a]

sterol ratio[b]	$t_{1/2}$ (h)
100:0	6.37 ± 0.48
90:10	4.73 ± 0.05
80:20	4.53 ± 0.02
70:30	3.55 ± 0.20
50:50	3.24 ± 0.54
20:80	2.69 ± 0.06
10:90	2.14 ± 0.30

[a] Vesicles were prepared with ePC/sterol = 1:1. Errors are standard deviation based on quadruplicate measurements with two independent preparations of vesicles. [b] Sterol ratio = % cholesterol/%cholest-4-en-3-one.

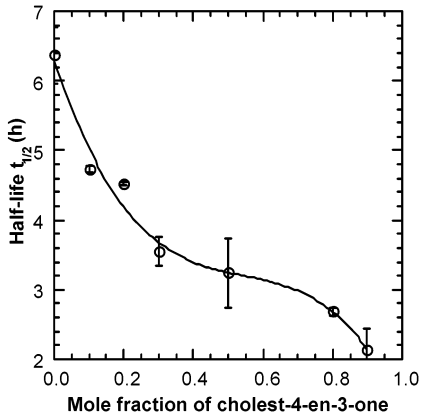

FIGURE 2: Dependence of half-life ($t_{1/2}$) for cholesterol transfer on mole fraction of cholest-4-en-3-one. Vesicles were ePC/steroid (1:1) and the steroid used was a binary mixture of cholesterol and cholest-4-en-3-one. The $t_{1/2}$ for cholesterol transfer was determined using the method of Hope (*28*). Errors are standard deviation based on quadruplicate measurements with two independent preparations of vesicles.

Steady-State Kinetics of Wild-Type Cholesterol Oxidase. The initial rate corresponding to the first 10% of total cholesterol conversion was measured as a function of cholesterol mole fraction ranging from 5 to 50%. A maximal v_i^{sat} representing the initial velocity when all the enzyme is bound to the vesicle was calculated from a binding isotherm of the observed v_i versus lipid concentration (eq 2). The K_{app} is the monomeric phospholipid concentration at which v_i is half-maximal. v_i was measured at two temperatures: 10 °C above and 10 °C below the T_m of DPPC. Catalase was added to the kinetic assays with DOPC/cholesterol vesicles to block the undesired peroxidation of oleolyl alkenes by H_2O_2. Light scattering intensities were measured for DOPC/cholesterol vesicles at $X_{chol} = 0.25$ and 0.40, and found to be the same within 4%.

In the case of DOPC, plots of v_i^{sat}/[E] versus mole fraction of cholesterol (X_{chol}) did not show a hyperbolic pattern for straightforward Michaelis−Menten treatment at either temperature (Figure 3A,B). The initial rate increased as the mole fraction of cholesterol increased, but was biphasic with an inflection point in v_i^{sat}/[E] at approximately $X_{chol} = 0.3$. For example, at $X_{chol} = 0.25$ and 31 °C, the initial rate was only 22% of the initial rate at $X_{chol} = 0.50$, whereas a

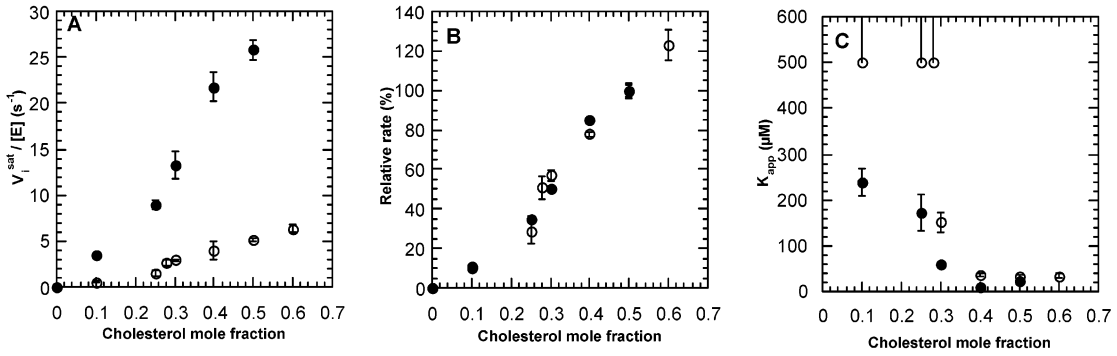

FIGURE 3: Steady-state rate measurements for DOPC/cholesterol vesicles. (A) Dependence of v_i^{sat}/[E] values of wild-type cholesterol oxidase on mole fraction of cholesterol. v_i^{sat}/[E] values at 31 °C (○), and 51 °C (●). (B) Relative-percent dependence of v_i^{sat}/[E] on mole fraction of cholesterol. v_i^{sat}/[E] at $X_{chol} = 0.5$ is normalized to 100% for each temperature, 31 °C (○), and 51 °C (●). (C) Dependence of K_{app} values on mole fraction of cholesterol, 31 °C (○), and 51 °C (●). The K_{app} and v_i^{sat}/[E] for $X_{chol} = 0.1$, 0.25, and 0.28 at 31 °C are only approximate because K_{app} was higher than the highest concentration of vesicles assayed (500 μM). Errors are standard deviation based on quadruplicate measurements with two independent preparations of vesicles.

Table 2: Second-Order Interfacial Rate Constants for Wild Type Turnover with 100-nm Vesicles[a]

	31 °C		51 °C	
lipid mole fraction of cholesterol	lipid phase	k^*_{cat}/K^*_m (mol fraction^{-1} s^{-1})	lipid phase (*21, 43*)	k^*_{cat}/K^*_m (mol fraction^{-1} s^{-1})
DOPC/cholesterol < 0.3	l_d low activity	8.33 ± 1.2	l_d low activity	35.9 ± 2.1
DOPC/cholesterol > 0.3	l_d high activity	11.5 ± 0.01	l_d high activity	62.5 ± 2.0
DPPC/cholesterol < 0.05	s_o	n.d.[b]	l_d	n.d.
DPPC/cholesterol > 0.05 < 0.3	s_o-l_o	3.4 ± 0.01	l_o-l_d	21.1 ± 0.9
DPPC/cholesterol > 0.3	l_o	6.5 ± 0.15	l_o	29.0 ± 0.35

[a] Errors are standard deviation based on quadruplicate measurements with two independent preparations of vesicles. [b] n.d.: not determined.

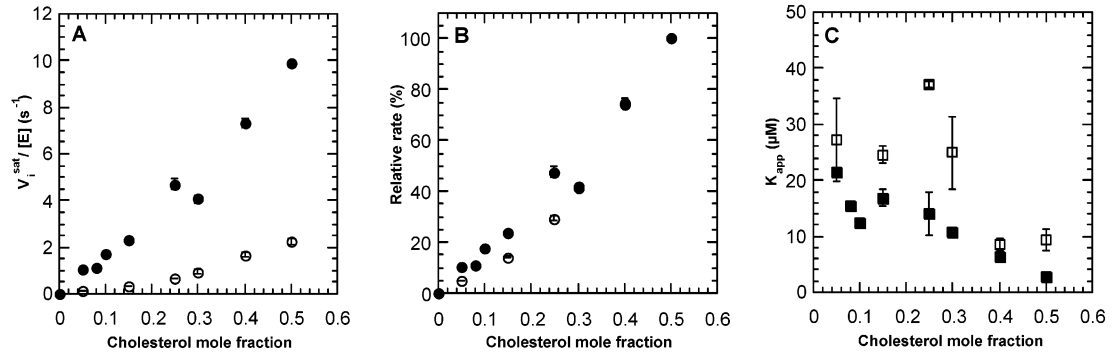

FIGURE 4: Steady-state rate measurements for DPPC:cholesterol vesicles. (A) Dependence of v_i^{sat}/[E] values of wild-type cholesterol oxidase on mole fraction of cholesterol. v_i^{sat}/[E] values at 31 °C (○), and 51 °C (●). (B) Relative-percent dependence of v_i^{sat}/[E] on mole fraction of cholesterol. v_i^{sat}/[E] at $X_{chol} = 0.5$ is normalized to 100% for each temperature, 31 °C (○), and 51 °C (●). (C) Dependence of K_{app} values on mole fraction of cholesterol, 31 °C (□), and 51 °C (■). Errors are standard deviation based on quadruplicate measurements with two independent preparations of vesicles.

hyperbola would predict the rate to be at least 50% of the $X_{chol} = 0.50$ value. These data suggest that there is a region of low cholesterol chemical activity below $X_{chol} = 0.3$ and a region of high cholesterol chemical activity above $X_{chol} = 0.3$. Moreover, it appears that in both regimes the enzyme is not saturated with substrate. Thus, we can only directly measure k^*_{cat}/K^*_m for each regime (Table 2). An approximately 5-fold increase in rate is observed with a 20 °C temperature increase regardless of mole fraction cholesterol compared. At 31 °C, the K_{app} for $X_{chol} = 0.1$, 0.25, and 0.28 could not be measured accurately because vesicle concentrations higher than 500 μM could not be used in the spectroscopic assay; 500 μM is a lower limit on the K_{app}. The changes in K_{app} as a function of DOPC/cholesterol mole fraction followed a trend similar to that of v_i^{sat}/[E] and decreased significantly as the mole fraction of cholesterol increased above 0.3 at both temperatures (Figure 3C). This trend also suggests that two states of substrate were assayed in the cholesterol range used.

In the case of DPPC/cholesterol vesicles, again no saturation of the enzyme is observed. The plots of v_i^{sat}/[E] versus mole fraction of cholesterol (X_{chol}) are linear in both the l_o regions and the coexistence regions (Figure 4A,B). Accurate kinetic measurements could not be obtained for the two phases, l_d and s_o, present below $X_{chol} = 0.05$, due to the low mole fraction of cholesterol and the low catalytic activity. Again, an inflection in activity as measured by both v_i^{sat}/[E]) and K_{app} occurred at $X_{chol} = 0.3$, the transition point between the l_o and the coexistence phases. However, the effect was much smaller than for DOPC:cholesterol vesicles.

Table 3: Dissociation Constants of H447E/E361Q Mutant for Binding to 100-nm Vesicles

	K_d (μM)[a]			
	DPPC/cholesterol		DOPC/cholesterol	
X_{chol}	31 °C	51 °C	31 °C	51 °C
0.50	8.81 ± 0.5	36.8 ± 11	24.0 ± 9.7	29.0 ± 4.3
0.25	4.90 ± 0.5	29.8 ± 4.2	23.8 ± 0.3	27.4 ± 0.4
0.05	1.50 ± 0.1	39.4 ± 5.6	24.0 ± 0.1	32.8 ± 5.2
0.00	<0.5	20.4 ± 10	19.4 ± 1.1	32.2 ± 2.5
0.00[b]	n.d.[c]	23.3 ± 0.3[b]	24.1[b]	n.d.

[a] Presented in monomeric lipid concentration for one binding site per lipid. Errors are standard deviation based on quadruplicate measurements with two independent preparations of vesicles. [b] K_d obtained with wild-type cholesterol oxidase. [c] Not determined.

k^*_{cat}/K^*_m was measured for each phase region (Table 2). An approximately 5-fold increase in rate is observed with a 20 °C temperature increase regardless of mole fraction cholesterol compared.

Binding Affinity of Cholesterol Oxidase for Lipid Vesicles. The change in cholesterol oxidase intrinsic tryptophan fluorescence emission upon binding to lipid vesicles (100 nm MUVs) was measured and fit to a binding isotherm (Table 3). There are 10 tryptophans in cholesterol oxidase. One on loop 73−86 is completely surface exposed, and four others are partially surface exposed. The quantum yield of tryptophan emission increased upon binding to lipid, consistent with a change from a hydrophilic to a hydrophobic environment. Dissociation constants are presented in monomeric lipid concentration, assuming one binding site per lipid molecule. Two phospholipid/cholesterol binary mixtures containing DOPC and DPPC, respectively, were used. Emission spectra were acquired at 31 and 51 °C to monitor the effect of the DPPC phase change (T_m of DPPC = 41 °C) (*25*). Analogous spectra of DOPC:cholesterol vesicles (T_m of DOPC = −16 °C) (*25*) were acquired as a control for temperature-dependent changes in enzyme behavior. As the cholesterol transfer experiments revealed that the product of cholesterol oxidase can alter the membrane structure, the H447E/E361Q mutant was used for the binding assay to block undesired conversion of cholesterol to cholest-4-en-3-one. The catalytic activity of the H447E/E361Q mutant was sufficiently low to perform the binding assay without cholest-4-en-3-one production (*26*).

The dissociation constants (K_d's) were measured for a range of cholesterol mole fractions for each temperature and phospholipid (Table 3). For DOPC/cholesterol vesicles, the K_d values were similar at 31 and 51 °C, ranging between 20 and 30 μM. However, the dissociation constants for DPPC/cholesterol vesicles at 31 °C were much lower than either the K_d's for DPPC/cholesterol at 51 °C or the K_d's for DOPC/cholesterol vesicles.

Only the dissociation constants for DPPC/cholesterol at 31 °C were strongly dependent on the mole fraction of cholesterol in the vesicle membrane. The K_d's decreased as the mole fraction of cholesterol increased. Dissociation constants for the other cases showed no direct dependence on the mole fraction of cholesterol. In the absence of a phase change, the temperature effect on the binding affinity of cholesterol oxidase to vesicles was negligible.

Scheme 2 : Kinetic Model for Interfacial Catalysis Based on ref *34*

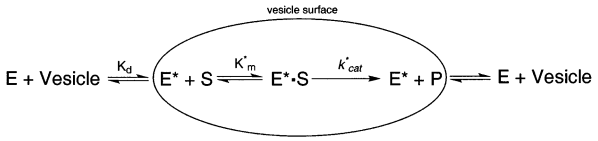

DISCUSSION

As an interfacial catalyst, cholesterol oxidase serves as a unique tool to probe the structure of lipid membranes using enzymatic activity as the detected signal. To recruit a cholesterol molecule into its active site, cholesterol oxidase must first interact with the membrane (Scheme 2). Three X-ray crystal structures of cholesterol oxidase have been solved: native *Brevibacterium* cholesterol oxidase (*choB*), *choB* enzyme complexed with dehydroepiandrosterone, a substrate analogue (*31*), and native *Streptomyces* cholesterol oxidase (*choA*) (*32*, *33*). Comparison of the X-ray structure of the free enzyme to the enzyme complexed with substrate analogue revealed that a conformational change must occur to expose the binding cavity to the membrane surface during steroid binding. Although the conformation of the "open" enzyme is not known, the structures suggest that one or two surface loops (residues 73−86, 432−438) open to form a hydrophobic pathway for the cholesterol molecule to move between the membrane and the active site. This lowers the activation barrier for cholesterol movement out of the lipid bilayer and facilitates transfer of cholesterol from the membrane to the active site of the enzyme and subsequent release of product. Mutagenesis of residues 79−83 (one part of the first loop) confirmed that it is important for binding substrate and for substrate specificity (*8*). Fluorescence binding measurements demonstrated that cholesterol oxidase physically sits on the surface of the membrane with loop 73−86 in contact, and that binding is primarily driven by hydrophobic interactions (*9*).

Reaction Progress Curves Are Sigmoidal. The kinetic activity profile of wild-type cholesterol oxidase using lipid bilayer substrates is sigmoidal as a function of time, rather than hyperbolic as expected for classical Michaelis−Menten behavior (Figure 1A). That is, after an initial lag phase, the initial velocity of the reaction becomes faster as the mole fraction of substrate in the membrane decreases. Previously, we determined that this was not due to a mixing phenomenon or slow binding of enzyme to the membrane surface (*10*). Interestingly, an active site mutant, E361Q, that produces cholest-5-en-3-one as the product rather than cholest-4-en-3-one shows hyperbolic behavior (Figure 1B). The E361Q reaction rate increases when cholest-4-en-3-one is added to the reaction mixture. This suggested to us that substrate binding or product release was partially rate-determining for both enzymes and that the sigmoidicity in the wild-type reaction was due to the formation and incorporation of the cholest-4-en-3-one product into the membrane. The two possible consequences of cholest-4-en-3-one presence in the membrane are an alteration in the enzyme affinity for the membrane surface, or a change in the cholesterol accessibility, i.e., stability in the membrane. For other interfacial enzymes, such as phospholipase A_2, changes in enzyme affinity for the membrane upon product formation are significant because the charge of the membrane surface

becomes anionic (*35*). In the case of cholesterol oxidase, the K_d for the membrane does not change significantly when cholest-4-en-3-one is incorporated (*10*). Thus, it appeared that the sigmoidal behavior was a consequence of cholest-4-en-3-one lowering the membrane affinity for cholesterol.

Cholesterol Transfer Rates Depend on the Mole Fraction of Cholest-4-en-3-one Present. To determine if cholest-4-en-3-one was modifying cholesterol stability in the membrane, we investigated whether the addition of cholest-4-en-3-one altered the rates of cholesterol exchange between membranes in the absence of cholesterol oxidase. There are two limiting mechanisms for lipid exchange or transfer between membrane bilayers that occur without specific protein or ionic interaction (*36*, *37*). One mechanism is an aqueous diffusion mechanism in which the lipids are transferred or exchanged through the aqueous phase. The second mechanism is a transient collision mechanism in which a collision between the membrane bilayers is critical for lipid transfer or exchange. Cholesterol exchange in model membrane unilamellar vesicles is first order with respect to the concentration of donor vesicles and zero order with respect to the concentration of acceptor vesicles when the acceptors are in excess (*38*, *39*). Thus, the transfer of cholesterol in this type of system occurs through monomer diffusion through the aqueous phase. Because the rate-determining step is desorption of cholesterol from the membrane layer into the aqueous state, half-lives of cholesterol transfer for different membrane compositions reflect the propensity with which cholesterol can leave the membrane.

We used the method of Hope (*28*) to measure the transfer rate of cholesterol out of cholest-4-en-3-one containing vesicles to determine the effect of cholest-4-en-3-one on steroid-lipid packing. We measured the transfer rate for a series of vesicles in which the phospholipid/steroid composition of the vesicles remained constant (1:1), and the mole fraction of steroid that was cholest-4-en-3-one versus cholesterol was varied. Donor and acceptor vesicles had the same lipid composition of egg phosphatidylcholine and steroid, except that lipid markers were different. We observed that inclusion of cholest-4-en-3-one in the lipid vesicles increases the rate of cholesterol transfer out of the vesicle (Figure 2). Thus, our hypothesis that cholest-4-en-3-one lowers the affinity of the membrane for cholesterol appeared correct. In other words, increasing amounts of cholest-4-en-3-one in the membrane increase the rate at which cholesterol moves out of the membrane even in the absence of cholesterol oxidase. Interestingly, the rate of cholest-4-en-3-one transfer was sufficiently fast ($t_{1/2} < 5$ min) that we could not obtain accurate transfer rates for the ketosteroid.

This change in cholesterol affinity explains the sigmoidal activity seen with wild type and the hyperbolic activity observed with the E361Q mutant. When cholesterol oxidase converts cholesterol into cholest-4-en-3-one, the membrane structure is altered and the partitioning of cholesterol into the active site of cholesterol oxidase is more favorable. This is consistent with a model in which cholesterol oxidase passively extracts cholesterol from the membrane. Consequently, enzyme activity is dependent on the structure of the lipid. However, as the rate of cholest-4-en-3-one transfer between vesicles is so fast, it is not possible to determine whether the product, cholest-4-en-one is released to the aqueous phase, directly returns to the membrane where the substrate cholesterol is obtained, or if it is returned to a different vesicle.

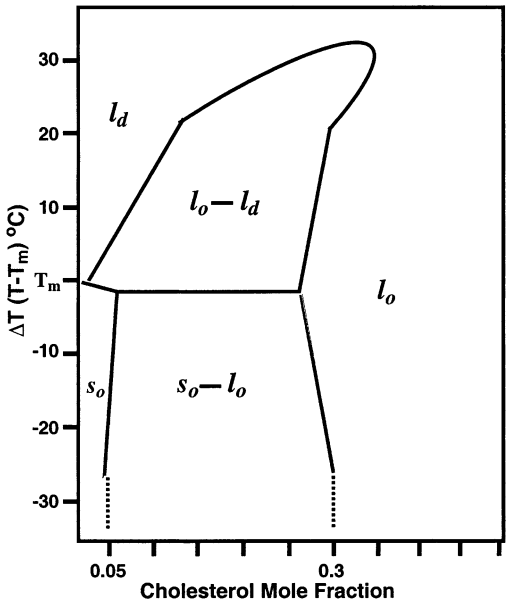

FIGURE 5: Temperature-composition phase diagram of the phospholipid−cholesterol system based on experimental data for DPPC/cholesterol and adapted from ref *21*.

The cholesterol oxidase activity profile in combination with our cholesterol transfer data suggest that cholesterol oxidase can sense subtle packing changes in the lipid membrane. Xu and London (*40*) have demonstrated that cholest-4-en-3-one is a raft dissolving steroid, that is, its behavior is very different than that of cholesterol. Whereas in ternary mixtures of DOPC, DPPC, and steroid, cholesterol will favor the formation of the l_o phase, cholest-4-en-3-one favors the l_d phase. Thus, the kinetic activity of cholesterol oxidase should be sensitive to the differences between the l_o and the l_d phases as well. Therefore, we undertook activity measurements with a variety of lipid structures.

Cholesterol Oxidase Binds Preferentially to the Solid Phase. Because the enzyme is water soluble and reversibly associates with the lipid membrane, care must be taken to measure the quantity of enzyme bound to the membrane in addition to making activity measurements. The phase diagram for binary mixtures of DPPC/cholesterol vesicles has been determined (*21*), and it has been suggested that the phase diagrams for other phospholipid and sphingolipid cholesterol mixtures have a nearly identical overall shape (*20*−*22*). According to this phase diagram, there are three one-phase regions and two two-phase coexistence regions. The three homogeneous phases are solid-ordered (s_o), liquid-ordered (l_o), and liquid-disordered (l_d). In the two-phase coexistence regions, the liquid-ordered (l_o) phase exists together with the other two phases. They are, respectively, the s_o-l_o phase and the l_o-l_d phase (Figure 5). We chose four mole fractions of cholesterol, 0.0, 0.05, 0.25, and 0.50 and monitored the binding affinity of cholesterol oxidase for MUVs at two temperatures, 10 °C above and 10 °C below the T_m of DPPC (41 °C), respectively. DOPC/cholesterol MUVs were also prepared and used in the binding assay under the same conditions as a control for temperature effects on the behavior of cholesterol oxidase. As the T_m of DOPC is −16 °C, the phase of DOPC/cholesterol MUVs should

remain in the liquid-disordered (l_d) state under our experimental conditions.

We utilized the H447E/E361Q double mutant of cholesterol oxidase because the catalytic activity of this mutant is reduced nearly 2500-fold compared to wild type (*26*). Thus, the binding assay could be executed without the disturbing effect of cholesterol conversion to cholest-4-en-3-one. The dissociation constants (K_d's) of the H447E/E361Q double mutant and wild type were found to be similar on nonsterol-containing membranes (Table 3, (*26*)), confirming that this double mutant is suitable for cholesterol oxidase binding experiments with lipid vesicles.

As shown in Table 3, the dissociation constants of mutant (H447E/E361Q) for DOPC/cholesterol MUVs at both 31 and 51 °C and the K_d's for DPPC/cholesterol MUVs at 51 °C were similar, ranging between 20 and 40 μM, regardless of the cholesterol mole fraction and temperature. In contrast, the K_d values for DPPC/cholesterol MUVs at 31 °C were much lower compared to the other conditions and were also dependent on the mole fraction of cholesterol in the membrane. According to the phase diagram from Sankaram and Thompson ((*21*), Figure 5), these lipid bilayer DPPC/cholesterol vesicles at $X_{chol} = 0$ to 0.5 at 31 °C are in rigid, solidlike phases (s_o, s_o-l_o phases).

Thus, we conclude that the binding affinity of cholesterol oxidase shows two trends. When the phase of the phospholipid:cholesterol membrane is in a liquidlike, fluid phase (l_o, l_d, and l_d-l_o coexistence phase), the binding affinities of cholesterol oxidase to the vesicles are similar with K_d values between 20 and 40 μM, regardless of phospholipid chain length or degree of saturation, or cholesterol amounts in the membrane. This conclusion also fits with data from our previous studies (*10*). Cholesterol oxidase binding affinities for unilamellar vesicles composed of ePC or POPC mixed with cholesterol were between 20 and 40 μM at 25 °C. As the T_m of ePC is −15 °C and the T_m of POPC is −5 °C (*25*), vesicles made of cholesterol and ePC or POPC are in a fluid phase at 25 °C. On the other hand, cholesterol oxidase binds with higher affinity to vesicle membranes that have a more ordered, tightly packed lipid structure. As the addition of cholesterol increases the percentage of liquid-ordered membrane in the coexistence phase region, the binding affinity decreases, approaching the binding affinities seen for purely fluid membranes. Although the physical model for this trend is unclear, it is consistent with the behavior of several polyene macrolide compounds that bind sterols, including filipin, nastatin, and amphotericin B. They all incorporate more extensively into membranes in the solid (gel) phase than into fluid phase membranes (*41*, *42*).

Steady-State Kinetic Rate Constants Depend on Lipid Structure. Heterogeneous catalysis mediated by an aqueous soluble enzyme with a substrate in the cell membrane is far more complex than homogeneous catalysis with soluble substrates. As membrane-bound substrates are constrained within the two-dimensional membrane, catalysis occurs at the heterogeneous interface between enzyme and membrane. Consequently, there is an additional binding step, binding of enzyme to the membrane, that must occur before substrate can bind in the active site. Thus, increasing the amount of vesicle added to the enzyme solution merely shifts the equilibrium between free enzyme, E, and enzyme at the interface, E* (Scheme 2). The mole fraction of substrate presented to the enzyme is not altered. We measured initial velocities (v_i) corresponding to the initial 10% of total cholesterol conversion, rather than entire progress curves (as has been utilized for phospholipases) because of our finding that the product cholest-4-en-3-one alters the membrane structure in which the substrates are dissolved. These initial velocities were measured for cholesterol mole fractions ranging from 0.05 to 0.50. v_i^{sat} is the initial velocity when all of the enzyme is bound to the vesicle surface at a fixed mole fraction of substrate, and is equivalent to an initial velocity measured for a soluble enzyme with soluble substrate at a fixed substrate concentration. K_{app} is the apparent equilibrium constant for saturating the initial velocity and represents a coupled equilibrium for enzyme-membrane (K_d) and enzyme−substrate (K_m^*) binding. For each mole fraction of cholesterol studied, we measured initial velocity, v_i, as a function of lipid concentration, and fit the activity data to eq 2. At each cholesterol mole fraction, we determined v_i^{sat} and K_{app}. If the lipid phase remained constant across all X_{chol} for which activity data were obtained, we expected that a plot of v_i^{sat}/[E] versus X_{chol} would be analogous to a solution phase Michaelis−Menten treatment.

At both temperatures for which we measured rates, lipid bilayers of DOPC/cholesterol are only one phase (liquid-disordered) regardless of their cholesterol mole fraction (Figure 5). We chose this system to normalize for temperature effects on cholesterol oxidase activity as well as to determine the interfacial K_m^* of the enzyme in the liquid-disordered phase. As shown in Figure 3, the kinetics did not follow the expected Michaelis−Menten paradigm. At both temperatures, the enzyme activity decreased twice as much as expected when the X_{chol} dropped below 0.3. K_{app} also showed an inflection with a large increase below $X_{chol} = 0.3$ at both temperatures. On the basis of our model that cholesterol oxidase does not actively extract cholesterol from the membrane and our studies showing that the binding affinities of cholesterol oxidase for DOPC/cholesterol MUVs do not vary, it appears that the enzyme is detecting a structural change in the membrane that occurs when the mole fraction of cholesterol shifts above or below 0.3. This structural change affects both k_{cat}^* and K_m^* with a large increase in K_m^* occurring at low mole fractions of cholesterol.

This phenomenon is consistent with the observation of Radhakrishnan and McConnell and co-workers that the chemical activity of cholesterol in monolayers significantly increases when the mole fraction of cholesterol rises above 0.3 (*43*, *44*). Chemical activity refers to the tendency of cholesterol to escape from the membrane. In an ideal, homogeneous two-dimensional membrane, the probability of a cholesterol molecule leaving the membrane should be directly proportional to the mole fraction of cholesterol in the membrane. Radhakrishnan and McConnell's monolayer studies, however, suggest that the probability can be further reduced by the formation of lipid complexes of cholesterol and phospholipids. Thus, the flux of cholesterol escaping from the membrane is proportional to the concentration of "free" rather than total cholesterol. They calculated the theoretical chemical activity in a homogeneous membrane as a function of cholesterol concentration (*44*). A sharp increase in cholesterol chemical activity is predicted and

observed at $X_{chol} = 0.33$. This suggests that the phospholipid complexes with cholesterol in a 2:1 molar ratio. As cholesterol is added to the membrane in excess of this ratio, the free cholesterol concentration increases and the cholesterol chemical activity increases.

We conclude that the behavior of $v_i^{sat}/[E]$ and K_{app} as a function of cholesterol mole fraction in DOPC bilayers is due to the change of cholesterol chemical activity in the vesicle membranes at $X_{chol} = 0.33$. McConnell's model demonstrates an approximately 2-fold increase in cholesterol chemical activity above $X_{chol} = 0.33$, and we observe a 2-fold increase in rate constant, suggesting that the rate is linearly dependent on chemical activity. Thus, our experiments provide a correlation between previous observations in monolayers and the behavior of cholesterol in lipid bilayers. Feigenson and co-workers have suggested that similar types of bilayer effects occur at higher mole fractions of cholesterol as the cholesterol reaches maximum solubility in the lipid bilayer at $X_{chol} = 0.66$ with phosphatidylcholines (*45*, *46*). They further demonstrate that improper sample preparation has led to cholesterol/phospholipid demixing and artificially low estimates of the solubility of cholesterol in the bilayer. We monitored our vesicle preparations by light scattering as described (*45*), both above and below the observed $X_{chol} = 0.3$ transition point, and saw no evidence of cholesterol crystallinity at $X_{chol} = 0.3$ as the scattering intensities remained constant. It appears, therefore, that the changes in bilayer structure occurring in the l_d phase at $X_{chol} = 0.3$ are not due to cholesterol precipitation, i.e., insolubility, but result from a less dramatic change in packing order as proposed by Radhakrishnan and McConnell.

Dissociation constants for binding of cholesterol oxidase to vesicles composed of very low T_m phospholipid and cholesterol at room temperature (to reduce catalytic turnover) are the same as those observed in observed in this work for our catalytically inactive mutant H447E/E361Q at higher temperatures (*10*). Consequently, we can assume that K_d, the affinity of the enzyme for the vesicle, does not change when cholesterol is bound in the active site, and we can approximate changes in K_m^* from changes in K_{app}. On the basis of these assumptions, the interfacial K_m^* is nearly 10-fold higher for low activity cholesterol in the l_d phase compared to high activity cholesterol. Thus, one reason for low enzymatic activity in these membrane systems is the unfavorable partitioning of cholesterol from the membrane into the active site.

As observed for DOPC/cholesterol bilayers, in DPPC/cholesterol bilayers there is an inflection in kinetic behavior at $X_{chol} = 0.3$ both above and below the T_m. This transition point corresponds to the phase change between l_o and s_o-l_o, or l_o and l_d-l_o at 31 and 51 °C, respectively. Moreover, inspection of the $v_i^{sat}/[E]$ versus X_{chol} plot (Figure 4A,B) again shows that the enzyme is never saturated with substrate. The measured K_{app}'s indicate that the interfacial K_m^* for these bilayers is most sensitive to the transition between s_o and l_o phases, although the difference is not as dramatic as for high and low chemical activity DOPC/cholesterol bilayers. That is, the interfacial K_m^* is approximately 3-fold higher in the s_o-l_o coexistence region than in the l_o phase.

Comparison of the second-order rate constants (k_{cat}^*/K_m^*) for different lipid mixtures reveals that cholesterol oxidase shows a 2-fold substrate specificity for cholesterol in the l_d phase of high cholesterol chemical activity over the l_o phase. Moreover, the enzyme is 2-fold more specific for cholesterol in the l_o phase than in the s_o phase. Likewise, there is 2-fold specificity for cholesterol in the high cholesterol chemical activity l_d phase over cholesterol in the low chemical activity l_d phase. However, the substrate specificities for cholesterol in the l_d phase of low cholesterol chemical activity and in the l_o phase are the same (Table 2). Because the enzyme is never saturated with substrate under the conditions investigated, comparing single observations of rate or initial velocity can lead to incorrect conclusions unless the compared rates are measured at the same mole fraction of cholesterol.

Summary. We have investigated the dependence of cholesterol oxidase activity on lipid phase. The binding affinities of cholesterol oxidase for MUV mixtures of DOPC or DPPC and cholesterol are not sensitive to cholesterol mole fraction if the phase of the membrane is fluid, i.e., in a physiologically relevant state. When the membrane solidifies, the binding affinity of cholesterol oxidase increases. However, the more ordered the lipid cholesterol structure, the lower the catalytic rate. Monitoring the kinetic activity of cholesterol oxidase with various lipid phases and structures demonstrates that enzymatic activity directly reflects the facility with which cholesterol can move out of the membrane, whether changes in cholesterol transfer facility are due to phase changes or more localized changes in packing. We conclude that the activity of cholesterol oxidase is directly and sensitively dependent on the physical properties of the membrane in which its substrate is bound. Future studies will further address the effect of changing lipid structure on cholesterol oxidase activity in lipid bilayers. Although it will be difficult to make meaningful biophysical measurements on cell membranes that contain complex mixtures of different lipid domains, single molecule technology may provide entry to experiments that employ cholesterol oxidase activity as a useful tool to detect microdomains in cellular membranes.

ACKNOWLEDGMENT

We thank Prof. Erwin London for scientific advice and critical reading of the manuscript.

REFERENCES

1. Greenplate, J. T., Duck, N. B., Pershing, J. C., and Purcell, J. P. (1995) Cholesterol oxidase − an oostatic and larvicidal agent active against the cotton boll-weevil, *Anthonomus-grandis*. *Entomol. Exp. Appl. 74*, 253−258.
2. Purcell, J. P., Greenplate, J. T., Jennings, M. G., Ryerse, J. S., Pershing, J. C., Sims, S. R., Prinsen, M. J., Corbin, D. R., Tran, M., Sammons, R. D., and Stonard, R. J. (1993) Cholesterol oxidase: a potent insecticidal protein active against boll weevil larvae. *Biochem. Biophys. Res. Commun. 196*, 1406−13.
3. Fernandez-Garayzabal, J. F., Delgado, C., and Dominguez, L. (1996) Cholesterol oxidase from *Rhodococcus equi* is likely the major factor involved in the cooperative lytic process (CAMP reaction) with *Listeria monocytogenes*. *Lett. App. Microbiol. 22*, 249.
4. Navas, J., Gonalez-Zorn, B., Ladron, N., Garrido, P., and Vazquez-Boland, J. A. (2001) Identification and mutagenesis by allelic exchange of *choE*, encoding a cholesterol oxidase from the intracellular pathogen *Rhodococcus equi*. *J. Bacteriol. 183*, 4796−4805.
5. Av-Gay, Y., and Sobouti, R. (2000) Cholesterol is accumulated by mycobacteria but its degradation is limited to nonpathogenic fast-growing mycobacteria. *Can. J. Microbiol. 46*, 826−831.

6. Fielding, C. J., and Fielding, P. E. (2003) Relationship between cholesterol trafficking and signaling in rafts and caveolae. *Biochim. Biophys. Acta 78435*, 1−10.
7. Bar, L. K., Chong, P. L.-G., Barenholz, Y., and Thompson, T. E. (1989) Spontaneous transfer between phospholipid bilayers of dehydroergosterol, a fluorescent cholesterol analogue. *Biochim. Biophys. Acta 983*, 109−112.
8. Sampson, N. S., Kass, I. J., and Ghoshroy, K. B. (1998) Assessment of the role of an Ω loop of cholesterol oxidase: a truncated loop mutant has altered substrate specificity. *Biochemistry 37*, 5770−5778.
9. Chen, X., Wolfgang, D., and Sampson, N. S. (2000) Use of the parallax-quench method to determine the position of the active-site loop of cholesterol oxidase in lipid bilayers. *Biochemistry 39*, 13383−13389.
10. Ghoshroy, K. B., Zhu, W., and Sampson, N. S. (1997) Investigation of membrane disruption in the reaction catalyzed by cholesterol oxidase. *Biochemistry 36*, 6133−6140.
11. Grönberg, L., and Slotte, J. P. (1990) Cholesterol oxidase catalyzed oxidation of cholesterol in mixed lipid monolayers: effects of surface pressure and phospholipid composition on catalytic activity. *Biochemistry 29*, 3173−3178.
12. Slotte, J. P. (1992) Cholesterol oxidase susceptibility of cholesterol and 5-androsten-3β-ol in pure sterol monolayers and in mixed-monolayers containing 1-palmitoyl-2-oleoyl-*sn*-glycerol-3-phosphocholine. *Biochim. Biophys. Acta 1124*, 23−28.
13. Slotte, J. P. (1992) Enzyme-catalyzed oxidation of cholesterol in mixed phospholipid monolayers reveals the stoichiometry at which free cholesterol clusters disappear. *Biochemistry 31*, 5472−7.
14. Mattjus, P., and Slotte, J. P. (1994) Availability for enzyme-catalyzed oxidation of cholesterol in mixed monolayers containing both phosphatidylcholine and sphingomyelin. *Chem. Phys. Lipids 71*, 73−81.
15. Mattjus, P., Hedström, G., and Slotte, J. P. (1994) Monolayer interaction of cholesterol with phosphatidylcholines: effects of phospholipid acyl chain length. *Chem. Phys. Lipids 74*, 195−203.
16. Mattjus, P., and Slotte, J. P. (1996) Does cholesterol discriminate between sphingomyelin and phosphatidylcholine in mixed monolayers containing both phospholipids. *Chem. Phys. Lipids 81*, 69−80.
17. Bittman, R., Kasireddy, C. R., Mattjus, P., and Slotte, J. P. (1994) Interaction of cholesterol with sphingomyelin in monolayers and vesicles. *Biochemistry 33*, 11776−81.
18. London, E. (2002) Insights into lipid raft structure and formation from experiments in model membranes. *Curr. Opin. Struct. Biol. 12*, 480−6.
19. Visit, M. R., and Davis, J. H. (1990) Phase equilibria of cholesterol/dipalmitoylphosphatidylcholine mixtures: deuterium nuclear magnetic resonance and differential scanning calorimetry. *Biochemistry 29*, 451−464.
20. Sankaram, M. B., and Thompson, T. E. (1990) Interaction of cholesterol with various glycerophospholipids and sphingomyelin. *Biochemistry 29*, 10670−10675.
21. Sankaram, M. B., and Thompson, T. E. (1991) Cholesterol-induced fluid-phase immiscibility in membranes. *Proc. Natl. Acad. Sci. U.S.A. 88*, 8686−8690.
22. Mateo, C. R., Acuña, A. U., and Brochon, J.-C. (1995) Liquid-crystalline phases of cholesterol/lipid bilayers as revealed by the fluorescence of *trans*-parinaric acid. *Biophys. J. 68*, 978−987.
23. McMullen, T. P., and McElhaney, R. N. (1995) New aspects of the interaction of cholesterol with dipalmitoylphosphatidylcholine bilayers as revealed by high-sensitivity differential scanning calorimetry. *Biochim. Biophys. Acta 1234*, 90−98.
24. Brown, D. A., and London, E. (1998) Origin and structure of ordered lipid domains in biological membranes. *J. Membr. Biol. 164*, 103−114.
25. Silvius, J. R. (1982) in *Lipid−Protein Interactions*, John Wiley & Sons, Inc, New York.
26. Ye, Y., Liu, P., Anderson, R. G. W., and Sampson, N. S. (2002) Construction of a catalytically inactive cholesterol oxidase mutant: investigation of the interplay between active site residues glutamate 361 and histidine 447. *Arch. Biochem. Biophys. 402*, 235−242.
27. Sampson, N. S., and Chen, X. C. (1998) Increased expression of *Brevibacterium sterolicum* cholesterol oxidase in *Escherichia coli* by genetic modification. *Protein Exp. Purif. 12*, 347−352.
28. Hope, M. J., Bally, M. B., Webb, G., and Cullis, P. R. (1985) Production of large unilamellar vesicles by rapid extrusion procedure. Characterization of size distribution, trapped volume and ability to maintain a membrane potential. *Biochim. Biophys. Acta 812*, 55−65.
29. Stewart, J. C. M. (1980) Colorimetric determination of phospholipids with ammonium ferrothiocyanate. *Anal. Biochem. 104*, 10−14.
30. Smith, A. G., and Brooks, C. J. W. (1977) The substrate specificity and stereochemistry, reversiblility and inhibition of the 3-oxo steroid Δ^4-Δ^5 isomerase component of cholesterol oxidase. *Biochem. J. 167*, 121−129.
31. Li, J., Vrielink, A., Brick, P., and Blow, D. M. (1993) Crystal structure of cholesterol oxidase complexed with a steroid substrate: implications for flavin adenine dinucleotide dependent alcohol oxidases. *Biochemistry 32*, 11507−11515.
32. Yue, K., Kass, I. J., Sampson, N., and Vrielink, A. (1999) Crystal structure determination of cholesterol oxidase from *Streptomyces* and structural characterization of key active site mutants. *Biochemistry 38*, 4277−4286.
33. Lario, P., Sampson, N. S., and Vrielink, A. (2003) Sub-atomic resolution crystal structure of cholesterol oxidase: What atomic resolution crystallography reveals about enzyme mechanism and the role of the FAD cofactor in redox activity. *J. Mol. Biol. 326*, 1635−1650.
34. Berg, O. G., Gelb, M. H., Tsai, M. D., and Jain, M. K. (2001) Interfacial enzymology: the secreted phospholipase A(2)-paradigm. *Chem. Rev. 101*, 2613−54.
35. Gelb, M. H., Jain, M. K., Hanel, A. M., and Berg, O. G. (1995) Interfacial enzymology of glycerolipid hydrolases − lessons from secreted phospholipases A_2. *Annu. Rev. Biochem. 64*, 653−688.
36. Brown, R. E. (1992) Spontaneous lipid transfer between organized lipid assemblies. *Biochim. Biophys. Acta 1113*, 375−389.
37. Phillips, M. C., Johnson, W. J., and Rothblat, G. H. (1987) Mechanisms and consequences of cellular cholesterol exchange and transfer. *Biochim. Biophys. Acta 906*, 223−276.
38. Philips, M. C., Johnson, W. J., and Rothblat G. H. (1987) Mechanisms and consequences of cellular cholesterol exchange and transfer. *Biochim. Biophys. Acta 906*, 223−276.
39. Mclean, L. R., and Philips, M. C. (1984) Kinetics of phosphatidylcholine and lysophosphatidylcholine exchange between unilamellar vesicles. *Biochemistry 23*, 4624−4630.
40. Xu, X., and London, E. (2000) The effect of sterol structure on membrane lipid domains reveals how cholesterol can induce lipid domain formation. *Biochemistry 39*, 843−849.
41. Castanho, M. A., and Prieto, M. (1992) Fluorescence study of the macrolide pentaene antibiotic filipin in aqueous solution and in a model system of membranes. *Eur. J. Biochem. 207*, 125−134.
42. Castanho, M. A., Prieto, M., and Jameson, D. M. (1999) The pentaene macrolide antibiotic filipin prefers more rigid DPPC bilayers: a fluorescence pressure dependence study. *Biochim. Biophys. Acta 1419*, 1−14.
43. Radhakrishnan, A., and McConnell, H. M. (2003) Condensed complexes of cholestrerol and phospholipids. *Biochim. Biophys. Acta 1610*, 159−173.
44. Radhakrishnan, A., and McConnell, H. M. (2000) Chemical activity of cholesterol in membranes. *Biochemistry 39*, 8114−8124.
45. Huang, J., Buboltz, J. T., and Feigenson, G. W. (1999) Maximum solubility of cholesterol in phosphatidylcholine and phosphatidylethanolamine bilayers. *Biochim. Biophys. Acta 1417*, 89−100.
46. Huang, J., and Feigenson, G. W. (1999) A microscopic interaction model of maximum solubility of cholesterol in lipid bilayers. *Biophys. J. 76*, 2142−2157.

BI035697Q